Dirac-Weyl points' manipulation using linear polarised laser field in Floquet crystals for various graphene superlattices

Dirac-Weyl points' manipulation using linear polarised laser field in Floquet crystals for various Graphene superlattices

IOP Conf. Series: Journal of Physics: Conf. Series **961** (2017) 012012 doi:10.1088/1742-6596/961/1/012012

Dirac-Weyl points' manipulation using linear polarised laser field in Floquet crystals for various Graphene superlattices

S.A. Alfadhli[1,2], S.E. Savel'ev[1] and F.V. Kusmartsev[1]
[1]Department of Physics, Loughborough University, Loughborough LE11 3TU, United Kingdom
[2]Department of Physics, University of Tabuk, Tabuk, 71491, Saudi Arabia

Abstract. We investigate the changes in the energy spectrum of the graphene monolayer subjected to linear polarised laser beam and external periodically modulated static field (electric and magnetic). Floquet theory and the resonance approximation are used to analyse the energy spectrum and, in particular, the creation and the destruction of the Dirac-Weyl points. We found that at certain conditions the graphene is transformed into the two-dimensional Weyl metals, where each of the two original graphene Dirac cones is split into pairs of the Weyl cones. We also show that altering the laser's beam incidence(tilting) angle may lead to appearing and disappearing of the pairs of Weyl points, the opening gap in the spectrum, and its efficient manipulation.

1. Introduction

The two-dimensional nature of graphene discovered in 2004 has enlightened the importance of potential applications of the 2D crystals [1] [2] [3] [4]. The gapless energy structure of graphene allows the electrons to travel freely with a very high mobility [5] and small electrical resistance [6]. However, the optoelectronic application of graphene requires an opening energy gap in the Dirac spectrum. [7] [8] [9] [10] [11]. Specifically, for a transistor construction and its various application the gap should be opened and closed with very high gigahertz (GHz) or even terahertz (THz) frequency and that should be controlled by varying external circuit parameters [12] [13] [14]. One of the promising gap controlling techniques is a generation of periodic potential, i.e. the creation of the so-called graphene superlattices. Such devices may have a very high electric mobility [15] [16], that is a prerequisite for the Bloch oscillations [17] [18] [19] [20]. From other side that can provide a strong potential for numerous GHz and THz practical applications [21] [22] [21]. An analogy was found between this costly-delicate method and between graphene placed in laser fields [23] [24] [25] [26] [27]. The laser field provide very nontrivial changes with materials and especially with graphene and may be used to test novel topological phases. For example, an application of the laser field to epitaxial graphene grown on SiC subjected even to very weak magnetic field transforms it into topological insulator with very nontrivial topological phases [28]. Moreover, an application of both constant electrical and inhomogeneous or periodic magnetic field can create in graphene snake states which is a feature of another class of topological insulator, the topological classification, Class AII, $Z_2 = 1$ [29]. The similar situation arises when we apply a constant magnetic and periodic electrical field. In this case single layer graphenes have one-dimensional domain walls that can arise in the places where the electrical or magnetic field changes sign. There arise snake states induced by orbital quantization in the spatially varying perpendicular magnetic field. Thus the periodic potential, either electrical or magnetic form a superlattice of domain walls. Each domain wall may be viewed as a p-n junction, which has topologically protected states, where there are topologically protected orbital currents.

These confined electronic states may provide configurable transport channels for charge and spin. Transport through these domain wall channels and switching from the edge to the internal pathways can be in principle controlled by an electrostatic gate and the laser field. The periodic electrical potential can be provided e.g. by grain boundaries. That interfacial states on zero-angle grain boundaries are actually topologically protected zero modes that are protected by a novel nonlocal chiral symmetry of the graphene Hamiltonian near its charge neutrality point or the Dirac point. The significance of this nonlocality was shown for the first time in Ref. [29]. It was shown that the spectra for laterally confined states at p-n junctions and snake states for modulated B fields with uniform chemical potential are gauge equivalent representations of the same problem. When expressed in a Nambu particle-hole doubled representation the two problems are formally interconverted by a position-dependent particle-hole transformation. There ballistic transport through a gate defined p-n junction can be configured as a gate-tunable valley filter. Thus the system is very reach has numerous practical applications has a nonlocal symmetry and therewith is analogous to Weyl semi-metals [30], where Dirac-Weyl points may appear and disappear in pairs when the spatial inversion is broken. All these analogies are described in the recent review [31]. Having that in mind in this paper, we theoretically investigate the energy spectrum in single layered graphene superlattices controlled by the laser field, when simultaneously an external either electric or magnetic field is applied. Since the system has a very rich symmetry the application of the laser field can influence the number and the position of the Dirac point and in general change the energy spectrum. Indeed, we show that the spectra and the current flow of Dirac electrons in graphene can be controlled by altering the laser beam intensity and the incidence angle with respect to the graphene plane.

2. Modelling approach:

To describe the motion of electrons in graphene subjected to periodic time dependent and electro-magnetic field we use the 2D Dirac equation in the form [20]:

$$\left\{\vec{\sigma}.\left[\vec{p}\text{-}\vec{A}(t)\text{-}\vec{A}^{H}(x)\right]+U(x)\right\}\psi_{A,B}=\frac{i\partial\psi_{A,B}}{\partial t} \tag{1}$$

where $\vec{A}(t)$ is the part of the vector potential associated with the time dependent electric field, $\vec{A}^{H}(x)=\left(\vec{A}^{H}(x),\vec{A}_{y}^{H}(x)\right)$ is its magnetic part, $U(x)$ is a static electric field, and $\psi_{A,B}$ is the electron wave function represented by two components vector $\psi=\begin{pmatrix}\psi_A\\ \psi_B\end{pmatrix}$ referring to the electrons in the two triangular sublattices A and B, respectively. The expression (1) is written in units of $e=\hbar=v_F=1$. Floquet theory can be used to analyse an evolution of electron wave function in a periodic time dependent potential. It gives a solution in the form a "Bloch function" in the time domain: $\Psi(x,t)=e^{\text{-}i\varepsilon t}\Phi(x,t)$, where the function $\Phi(x,t)$ is periodic in time, $\Phi(x,t)=\Phi(x,t+T)$, and the value ε is the quasienergy or the Floquet energy. In the resonance approximation [20], where we are interesting only in the low-energy spectrum in a vicinity of the Dirac point of the graphene spectrum the wave function can be written as (e.g. see the Ref.[24], for a detail):

$$\psi_{A,B}=e^{\text{-}i\varepsilon t+ik_x x+ik_y y}\left[\psi_{A,B}^{++}\,e^{\frac{i\omega t}{2}+\frac{i\mu x}{2}}+\psi_{A,B}^{+\text{-}}\,e^{\frac{i\omega t}{2}\text{-}\frac{i\mu x}{2}}+\psi_{A,B}^{\text{-}+}\,e^{\frac{\text{-}i\omega t}{2}+\frac{i\mu x}{2}}+\psi_{A,B}^{\text{--}}\,e^{\frac{\text{-}i\omega t}{2}\text{-}\frac{i\mu x}{2}}\right] \tag{2}$$

where ω and μ are temporal frequency and spatial modulation inverse period of laser field and spatially-periodic static field (either electric or magnetic). We apply a linearly polarized laser field :

$$\vec{A}(t)_x=A_0 cos(\theta)cos(\omega t)\,;\,\vec{A}(t)_y=A_0 sin(\theta)cos(\omega t) \tag{3}$$

with the amplitude A_0 and polarization angle θ, which is the angle between the linear polarised laser field and the static field. First, we consider a case when magnetic part of the vector potential has the form, where $\vec{A}^{H}(x)_x=0, U(x)=0$. Then, we apply a static electric field oriented in the graphene plane. The field is associated with an electric potential of the form: $U(x)=U_0 cos(\mu x)$, where U_0 is the amplitude and μ is the value, inverse to the spatial modulation period, $d=2\pi/\mu$. In the considered case the electric field will be always in plane with the graphene sheet. Substituting the wave function and these potentials into the 2D Dirac equation (1) we obtain the following expressions:

$$i\frac{d}{dt}\begin{pmatrix}\phi_A\\ \phi_B\end{pmatrix}=\begin{pmatrix}U(x) & [\mathrm{p_x}\text{-}\mathrm{A_x}(t,x)]-i[\mathrm{p_y}\text{-}\mathrm{A_y}(t,x)]\\ [\mathrm{p_x}\text{-}\mathrm{A_x}(t,x)]+i[\mathrm{p_y}\text{-}\mathrm{A_y}(t,x)] & U(x)\end{pmatrix}\begin{pmatrix}\phi_A\\ \phi_B\end{pmatrix} \quad (4)$$

where $\mathrm{A(t,x)}=(\mathrm{A_x}(t,x),\mathrm{A_y}(t,x))=((\mathrm{A_x}(t)\text{-}\mathrm{A_x^H}(x),\ \ (\mathrm{A_y}(t)\text{-}\mathrm{A_y^H}(x)))$. By substitution of the expression for the truncated form of the wave function and neglecting the terms associated with higher order harmonics, we obtain the set of eight algebraic homogeneous equations, arranged in the form

$$\begin{bmatrix}
\frac{\omega}{2} & k_x-ik_y+\frac{\mu}{2} & C_nA_0 & 0 & C_mA_0^H & -\left(\frac{A_0}{2}\right)e^{-i\theta} & 0 & 0\\
k_x+ik_y+\frac{\mu}{2} & \frac{\omega}{2} & C_mA_0^H & C_nA_0 & -\left(\frac{A_0}{2}\right)e^{i\theta} & 0 & 0 & 0\\
C_nA_0 & C_mA_0^H & \frac{\omega}{2} & k_x-ik_y+\frac{\mu}{2} & 0 & 0 & 0 & -\left(\frac{A_0}{2}\right)e^{-i\theta}\\
C_mA_0^H & C_nA_0 & k_x+ik_y+\frac{\mu}{2} & -\frac{\omega}{2} & 0 & 0 & -\left(\frac{A_0}{2}\right)e^{i\theta} & 0\\
0 & -\left(\frac{A_0}{2}\right)e^{-i\theta} & 0 & 0 & -\frac{\omega}{2} & k_x-ik_y+\frac{\mu}{2} & C_nA_0 & C_mA_0^H\\
-\left(\frac{A_0}{2}\right)e^{i\theta} & 0 & 0 & 0 & k_x+ik_y+\frac{\mu}{2} & -\frac{\omega}{2} & C_mA_0^H & C_nA_0\\
0 & 0 & 0 & -\left(\frac{A_0}{2}\right)e^{-i\theta} & C_nA_0 & C_mA_0^H & -\frac{\omega}{2} & k_x-ik_y+\frac{\mu}{2}\\
0 & 0 & -\left(\frac{A_0}{2}\right)e^{i\theta} & 0 & C_mA_0^H & C_nA_0 & k_x+ik_y+\frac{\mu}{2} & -\frac{\omega}{2}
\end{bmatrix}\begin{bmatrix}\psi_A^{++}\\ \psi_B^{++}\\ \psi_A^{+-}\\ \psi_B^{+-}\\ \psi_A^{-+}\\ \psi_B^{-+}\\ \psi_A^{--}\\ \psi_B^{--}\end{bmatrix}=\varepsilon\begin{bmatrix}\psi_A^{++}\\ \psi_B^{++}\\ \psi_A^{+-}\\ \psi_B^{+-}\\ \psi_A^{-+}\\ \psi_B^{-+}\\ \psi_A^{--}\\ \psi_B^{--}\end{bmatrix} \quad (5)$$

Below we present the solution of this equation by setting its determinant equal to zero.

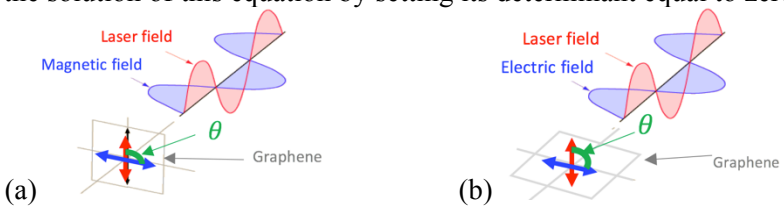

Figure 1. Schematic representation of the orientation set up for the discussed systems where a linearly polarized laser field applied in addition to an external spatially periodically modulated electric or magnetic field. (a) a static, periodically modulated magnetic field is applied perpendicular to the graphene sheet, while the polarisation of the laser field is applied at a chosen incidence angle θ with respect to the orientation of the static field. (b) a static, periodically modulated electric field is located in the graphene plane while a linear polarised laser field is tilted by angle θ with respect to the orientation of the electrical field.

3. Graphene in static magnetic and linear polarised laser field:

In this section we consider the case when the static magnetic field is applied perpendicular to the graphene sheet. Usually we should expect Landau Quantisation here and Landau spectrum consisting of Landau Levels if the spatial modulation period is very large. However, in additional linear polarised laser field and in the static field with the periodic spatial modulation the low energy spectrum from a first glance we see three Dirac points oriented parallel to k_x axes, when the wave vector $k_y = 0$ (see, the Figure 2). It is clear that this "tripling" is related to the spatial modulation of the magnetic field in x- direction which is creating domain walls parallel to the y- axes. However, a more precise inspection of this part of energy spectrum in the vicinity of the zero energy reveals that we have here two Dirac-Weyl points and one highly anisotropic gapless Dirac-like point at $\varepsilon = 0$, corresponding both, $k_x = 0$ and $k_y = 0$. The two Dirac-Weyl points shifted in the k_x direction correspond to the creation of the vortex and the anti-vortex in the energy-momentum space having the form of Dirac cones in the vicinity of the zero energy. When these cones are separated in the momentum space they are topologically protected and we cannot create a gap in the spectrum. But they can annihilate each other when you will be located at the same place and there an energy bandgap can be created. Note that the original Dirac point (in our notation here it is located at K or K' points of the Brillouin Zone but at the values, $k_x = 0$ and $k_y = 0$) is now strongly deformed and probably lost its linear character along k_x direction. The formation of the two Dirac-Weyl singularities in the vicinity of the K and K' points is a result of the dynamical topological phase transition created by an application of the both periodically modulated spatial and dynamical laser field. The position of these two Dirac-Weyl points can be

rotated by the changes of the angle between the laser field polarisation and the direction of the applied field of the periodic spatial modulation, see the Figure 3, where for an illustration the calculations have been done with the values of the parameters: $\omega = 1$, $\mu_H = 1$ and $A_0^H = 1$. From this Figure 3 we see that when the polarisation direction changes by $\pi/2$ the position of these two Weyl-Dirac points is perpendicular to their original orientation, when the direction of the laser field polarisation and of the modulated field coincide (see, the Figure 3).

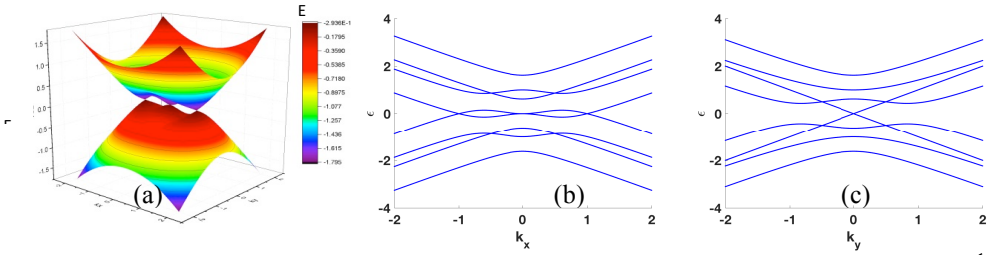

Figure 2. A three-dimensional plot and its cross sections of the energy spectrum $\varepsilon(k_x, k_y)$ of a single layered graphene obtained in the applied linearly polarised laser field together with a spatially-modulated periodic external magnetic field. The spectrum obtained with approximation strictly speaking valid only for the low energy $\varepsilon(k_x, k_y) < 1$. The calculation has been done with the parameters: $\omega = 1$, $\mu_H = 1$ and $A_0^H = 1$ for chosen fields orientations. (a) the spectrum shows two Dirac-Weyl points associated with Dirac cones and one highly anisotropic gapless point at $\varepsilon = 0$, corresponding both, $k_x = 0$ and $k_y = 0$. These two Dirac-Weyl points shifted in the k_x direction correspond to the creation of the vortex and the anti-vortex in the energy spectrum and are topologically protected. Interesting that the original Dirac point, which is in the present notation located at $k_x = 0$ and $k_y = 0$ is now strongly deformed and probably lost its linear character along k_x direction. Note that for graphene this Dirac point correspond to the K and K' points of the Brulluoen Zone. The formation of these two extra Dirac-Weyl cones in the vicinity of the K and K' points is a result of the dynamical topological phase transition created by an application of the both periodically modulated spatial and dynamical laser field. These two Dirac-Weyl points and one Dirac point are aligned along the k_x axes, i.e. at $k_y = 0$. On the Plot (b) we see this cross section while on the Plot (c) we present the cross section of the spectrum taken at $k_x = 0$.

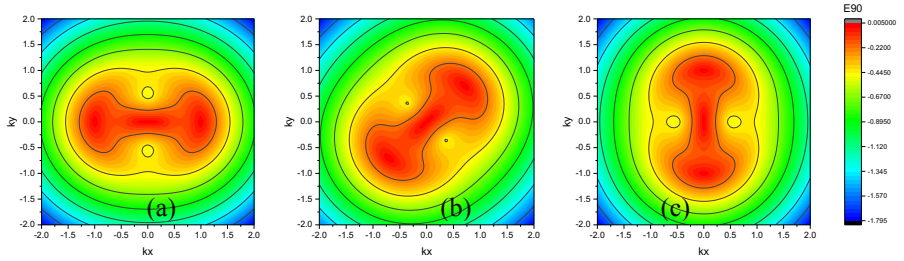

Figure 3. The contour Plot of the low-energy spectrum $\varepsilon(k_x, k_y)$ taken in the vicinity of each K and K' points of the Brillouin Zone for a single layered graphene in the perpendicular periodically modulated magnetic field and a linear polarised laser field tilted at different angles θ with respect to each other. (a) Shows the contour plot of the energy spectrum when $\theta = 0$, the symmetry axes of the spectrum is horizontally oriented parallel to k_x axis which coincides with the polarisation of the electromagnetic laser field. (b) As we rotate the laser field polarisation on $\theta = \pi/4$ or $\pi/2$ angle the Weyl Dirac points of the spectrum also rotates (see, the panels b and c).

4. Graphene in static electric and linear polarized laser field:

If we apply a static periodically modulated electric field and the linearly polarized laser field in the plane of the graphene sheet there are arise a two pairs of the Weyl-Dirac points. In this case when

$\theta = 0$ the energy spectrum shows that Dirac cones of graphene split into several mini bands (see, Figure 4-a). The case is very similar to the previous one, the spectrum has two Dirac-Weyl point and one central original Dirac point. However, the elongation of this central point is different, it occurs along k_y axes. All these points are located along the k_x axis and the spectrum seems to be gapless. The 3D plot (see, the Figure 4-b) shows the shape of these Dirac and Weyl cones and that the middle Dirac cone is elliptically shaped. When the angle θ changed from 0 to $\frac{\pi}{2}$, the number and positions of Dirac-Weyl points have changed to four (see, Figure 4-c), indicating a dynamical symmetry breaking phenomenon arising in the band structure with changes of the different laser beam orientations.

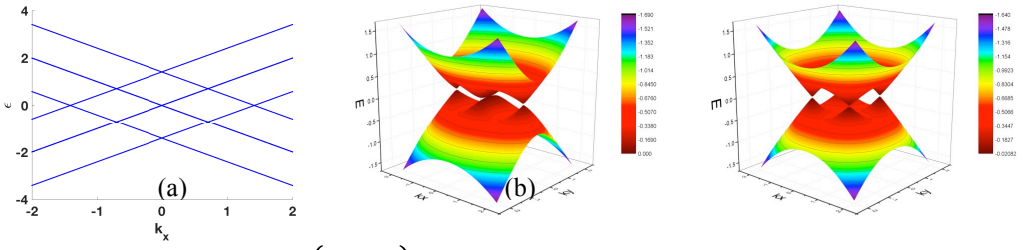

Figure. 4: Electron spectra $\varepsilon(k_x, k_y)$ for graphene subjected to linearly polarised laser fields with a static spatially-modulated periodic electric field. In the calculations we used the parameters $\omega = 1$, $\mu = 1$, $U_0 = 1$ and $A_0 = 1$ for each of chosen orientations, θ. (a) The spectrum shows gapless multiple crossing at the plane crossing the k_x axes. (b) showing two Weyl-Dirac located symmetrically with respect to the central Dirac point at K or K' place in the Brillouin Zone. All these three gapless points are oriented parallel to k_x at the value, $k_y = 0$. (c) The spectrum rotated by an angle equal to the laser's beam orientation, i.e., $\pi/2$, that is showing a broken special inversion symmetry and therewith forming two pairs of Weyl-Dirac cones symmetrically positioned around K or K' points of the Brillouin Zone.

To investigate in a detail the change in the spectrum, surface contour plots were shown at different laser field angles. For $\theta = 0$ there are three gapless points where the top and bottom energy bands touch each other. Near two peripheral points, the energy spectrum can be approximate as squeezed Dirac cones, $\varepsilon^2 = a\,(k_x)^2 + b(k_y)^2$, while near the middle point, the structure reminds a "cut" with energy $\varepsilon^2 = a(k_x)^2 + b(k_y)^4$, where a and b some real parameters. As the laser is rotating, two changes occur: 1)- the spectrum is rotating in a similar manner and 2)- the middle point experience a splitting where the energy cut transforms into two squeezed cones, see, the Figure 5-b, where the laser is applied at $\theta = \pi/4$. There spectrum has 4 Dirac points. When the laser field orientation changes, at the perpendicular case, when $\theta = \pi/2$, the spectrum is rotated by $\pi/2$ forming 4 Dirac-Weyl cones symmetric about the pole (see, the Figure 5-c), which is associated with K or K' of the graphene Brulloen Zone.

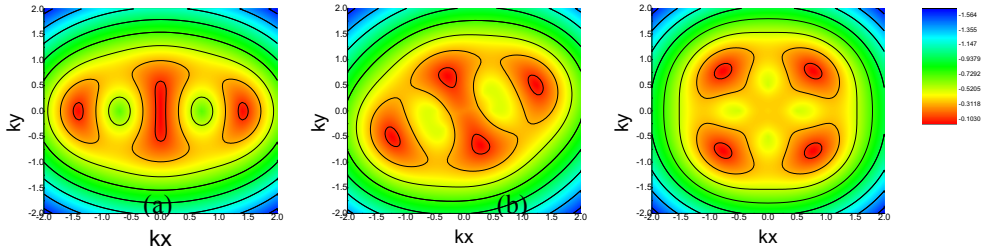

Figure. 5: The surface contour plot of the energy-momentum dispersion, $\varepsilon(k_x, k_y)$, for a monolayer graphene subjected to in-plane static periodically modulated electric field and a linear polarised laser field tilted at the angle θ to the graphene plane: (a) the case when the polarisation of the electromagnetic laser field coincides with the direction of the modulated electrical field, i.e. $\theta = 0$; Here we see a pair of the Weyl points located far apart from each other. In a centre there is an

elongated valley where a new pair of Weyl points is going to be nucleated, when the tilting angle increases, i.e. when $\theta \neq 0$; (b) The snapshot of the spectrum taken when the tilting angle $\theta = \pi/4$; We see already two pairs of the Weyl points here (c) The snapshot spectrum displaying two symmetrical pairs of the Weyl points taken at their perpendicular orientation, i.e. at $\theta = \pi/2$.

5. Conclusion

Here we shown that static periodically modulated magnetic/electric field together with linearly polarised laser field induce dynamical topological phase transitions in a single graphene layer. There in the vicinity of the original K and K' Dirac points the pairs of Weyl-Dirac cones are created. Then the graphene layer may be viewed as two-dimensional Weyl metal. The created Weyl metal energy spectrum is invariant under the laser field rotation when there is only spatial modulation of magnetic field. However, when the static electric field is periodically modulated, the system shows additional symmetry breaking phenomenon where additional pairs of the Weyl-Dirac cones are created. We show that this effect is controlled by a laser field tilting from the graphene plane where the modulated electric field is embedded. We expect that the described effect may be used in novel optoelectronic devices and the predicted phenomena will be observed in the future experiments.

References

[1] Novoselov, K S ; Geim, A K et al (2004), Science, 306(5696), 666-669.
[2] Meyer, J C ; Geim, A K ; et al (2007). Nature, 446, 60.
[3] O'hare, A., Kusmartsev, F. V., & Kugel, K. I. (2012). Nano letters, 12(2), 1045-1052.
[4] Geim , A. K. and Novoselov, K. S. (2007) The rise of graphene, *Nature Mater* 6, 183.
[5] Wallace, P. R (1947) Band theory of graphite, *Phys. Rev*. 71, 622.
[6] Yung, K. C., Wu, W. M., Pierpoint, M., & Kusmartsev, F. V. (2013). *Contemp. Phys.*, *54*, 233.
[7] Kusmartsev, F. V. and A. M. Tsvelik,(1985) JETP Lett., 42, 257-260.
[8] Pei, S., & Cheng, H. M. (2012). The reduction of graphene oxide. Carbon, 50(9), 3210-3228
[9] Georgakilas, V et al, (2012). Chemical Reviews, 112, 6156-6214.
[10] Bai, J. et al, (2010). Graphene nanomesh. Nature nanotechnology, 5(3), 190-194.
[11] Fang, T., et al. (2008). Physical Review B, 78(20), 205403.
[12] Rozhkov, A. V., Savel'ev, S., & Nori, F. (2009). Physical Review B, 79(12), 125420.
[13] Quhe, et al, (2012). NPG Asia Materials, 4, e6.
[14] Lu, T. M.,(2016). Scientific reports, *6. 20967*.
[15] Choi, S. M., Jhi, S. H., & Son, Y. W. (2010). Physical Review B, 81(8), 081407.
[16] Bliokh, Y. P., Freilikher, V., Savel'ev, S., & Nori, F. (2009). Physical Review B, 79(7), 07512
[17] Pedersen, T. G., et al. (2008). Physical Review Letters, 100(13), 136804
[18] Song, J. C., Shytov, A. V., & Levitov, L. S. (2013). Physical review letters, 111(26), 266801
[19] Alekseev, K. N., et al, (1998). Physica D: Nonlinear Phenomena, 113(2-4), 129-133
[20] Alekseev, K. N., et al . (1998). Phys. Rev. Lett., *80*(12), 2669.
[21] Alexeeva, N.; et al.,(2012) Phys. Rev. Lett., 109, 024102.
[22] Hramov, A. E., et al (2014). Phys. Rev. Lett., *112*(11), 116603.
[23] Savel'ev, S. E., & Alexandrov, A. S. (2011). Physical Review B, 84(3), 035428
[24] Rodriguez-Lopez, P., Betouras, J. J., & Savel'ev, S. E. (2014). Dirac fermion time-Floquet crystal: manipulating Dirac points. Physical Review B, 89(15), 155132
[25] Xia, F., Farmer, D. B., Lin, Y. M., & Avouris, P. (2010).Nano letters, 10(2), 715-718
[26] Zhang, Y., et al (2009). Nature, 459(7248), pp.820-823.
[27] Oostinga, J. B.,et al. *Nature Materials 7*(2), 151 – 157.
[28] Trabelsi, A. B. G.,et al. (2017). Nanoscale, 9, 11463-11474.
[29] Liu Yang, et al. (2015). Phys. Rev. B 92, 235438.
[30] R. D. Y. Hills, A. Kusmartseva, and F. V. Kusmartsev, (2017). , Phys. Rev. B 95, 214103.
[31] A. Kusmartseva and F. Kusmartsev (2017). Topological Materials: from polyacetylene to topological insulators and Weyl semimetals, Eur. Phys. J. B:-Conden.Matter Complex Syst. 90, 0001.